Self-Assembly of Monatomic Complex Crystals and Quasicrystals with a Double-Well Interaction Potential

Michael Engel* and Hans-Rainer Trebin
Institut für Theoretische und Angewandte Physik, Universität Stuttgart, Pfaffenwaldring 57, 70550 Stuttgart, Germany

For the study of crystal formation and dynamics we introduce a simple two-dimensional monatomic model system with a parametrized interaction potential. We find in molecular dynamics simulations that a surprising variety of crystals, a decagonal and a dodecagonal quasicrystal are self-assembled. In the case of the quasicrystals the particles reorder by phason flips at elevated temperatures. During annealing the entropically stabilized decagonal quasicrystal undergoes a reversible phase transition at 65% of the melting temperature into an approximant, which is monitored by the rotation of the de Bruijn surface in hyperspace.

PACS numbers: 61.50.Ah, 02.70.Ns, 61.44.Br, 64.70.Rh.

Self-assembly is the formation of complex patterns out of simple constituents without external interference. It is a truly universal phenomenon, fundamental to all sciences [1]. Although usually the constituents interact only locally, the result is well-ordered over long distances, sometimes with a high global symmetry. In the process of crystallization, particles (atoms, molecules, colloids, etc.) arrange themselves to form periodic or quasiperiodic structures. Here we are interested in structurally complex phases. Examples are metallic crystals with large unit cells – hundreds or thousands of atoms – known as complex metallic alloys [2]. Some consequences of the complexity are the existence of an inherent disorder and the formation of well-defined atomic clusters [3]. Related alloys differ by the cluster arrangement. In the limit of infinitely large unit cells non-periodic order like in quasicrystals [4] is obtained. However self-assembly of complex phases is not unique to alloys. Recently micellar phases of dendrimers were observed to form a mesoscopic quasicrystal [5], and there are indications that quasicrystals exist in monodisperse colloidal (macroscopic) systems [6]. Since the interaction between colloidal particles can be tuned in various ways, these systems are well-suited for experiments investigating self-assembly in dependence of the potential shape.

All of the previous examples have in common that the crystal growth can be modeled with effective pair potentials, which is a prerequisite for simulating self-assembly of a large number of particles on a computer. The first such simulations were conducted by Lançon and Billard in two [7] and by Dzugutov in three dimensions [8]. In the latter work the system was chosen monatomic to facilitate computation and separate chemical from topological ordering. It is well-known that many common pair-potentials like the Lennard-Jones (LJ) potential favor close-packed ground states. To force the formation of alternative structures the Dzugutov potential is endowed apart from its LJ minimum with an additional maximum. Although the potential was originally tailored to lead to a glassy state [8], it stabilizes the σ-phase at low temperature [9]. Later, similar potentials were used to demonstrate the formation of a dodecagonal quasicrystal in two dimensions [10], which on closer inspection was identified as a periodic approximant. In fact it is often difficult to distinguish quasicrystals and closely related periodic complex crystals due to their structural similarity.

The relation between an interaction potential and its energetic ground state is a fundamental problem of physics. It can be approached by two methods: The direct method starts from a given parametrized set of potentials and studies the resulting structures as a function of the parameters (and temperature/pressure). An example is the hard core plus linear ramp model with the ramp slope as single parameter [11]. The inverse method tries to find an appropriate potential that stabilizes a given structure via optimization [12]. It was used recently by Rechtsman et al. to find potentials for various lattices [13]. In this Letter we apply the direct method to a potential of the form [12]

$$V(r) = \frac{1}{r^{12}} - \frac{2}{r^6} - \epsilon \exp\left(-\frac{(r-r_0)^2}{2\sigma^2}\right), \qquad (1)$$

which we denote Lennard-Jones-Gauss (LJG) potential. For most values of the parameters $V(r)$ is a double-well-potential with the second well at position r_0, of depth ϵ and width σ (Fig. 1). We note that the general form of pair potentials in metals consists of a strongly repulsive core plus a decaying oscillatory (Friedel) term [14]. A LJG-potential can be understood as such an oscillatory potential, cut off after the second minimum.

In the following we restrict the parameter space by fixing $\sigma^2 = 0.02$. The $T = 0$ phase diagram in the r_0-ϵ-plane is determined in two steps: First, candidate ground state structures are obtained from annealing simulations. Next, a defect free sample of each candidate structure is relaxed with a conjugate gradient algorithm. During the relaxation particle movements and adjustments of the simulation box dimensions are allowed. The stable structures (within the candidates) are the ones with the lowest potential energies. Simulations were carried out by

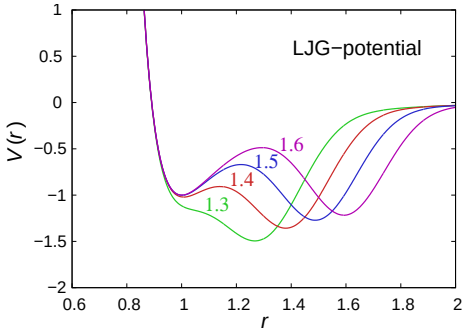

FIG. 1: (color online) LJG-potential for $\epsilon = 1.1$, $\sigma^2 = 0.02$, and $r_0 = 1.3$ (Hex2 in Fig. 2), 1.4 (Sqa), 1.5 (Pen), 1.6 (Hex1).

solving the equations of motion with molecular dynamics. Periodic boundary conditions and a Nosé-Hoover thermo-/barostat for constant temperature T and constant pressure $P = 0$ were used. A cut-off was applied to the LJG-potential at $r = 2.5$.

We performed 5000 annealing simulations with a sample of 1024 particles using parameters located on a fine grid: $r_0 \in [1.11, 2.10]$, $\Delta r_0 = 0.01$ and $\epsilon \in [0.1, 5.0]$, $\Delta\epsilon = 0.1$. During each run the temperature was lowered linearly over $2 \cdot 10^6$ molecular dynamics steps starting from the liquid state. A typical final particle configuration consists of several well-ordered grains whose structure is analyzed in direct and in reciprocal space. The phase observation regions are displayed in Fig. 2. We found hexagonal phases with nearest-neighbor distance close to 1.0 (Hex1) and close to r_0 (Hex2), a square lattice (Sqa), a decagonal (Dec) and a dodecagonal (Dod) quasiperiodic random tiling (RT), a phase built from pentagons and hexagons (Pen), a rhombic lattice (Rho), and finally a honeycomb lattice (Hon). It can be seen in Fig. 2 that the two hexagonal phases are connected around the phase Sqa. Across the line between C and the phase Sqa there is a rapid increase in the hexagonal lattice constant.

The phases resulting from the annealing simulations are possible energy ground states. Further possibilities are approximants, which we constructed from the tiles in Fig. 2. The choice of approximants is restricted by the following observations at low temperature: (i) The D-tiles have lowest energy and their number is maximized (see below). (ii) The Sh-tiles and two neighboring Sq-tiles are avoided. Together, the approximants and the phases from annealing simulations were used as initial structures for numerical relaxation. In the phase diagram (Fig. 3) five complex crystals are stable: the phase Pen, the decagonal approximant (Xi), which is a periodic stacking involving D-tiles, and three dodecagonal approximants: the σ-phase (Sig1) and two modifications (Sig2), (Sig3). Here we use the term "complex" since the lattice constants are larger than the potential cut-off, which means that the unit cells have to be stabilized indirectly

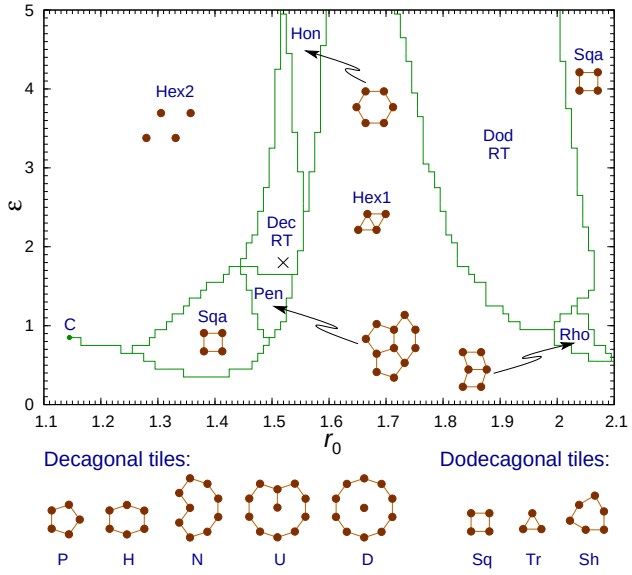

FIG. 2: (color online) Phase observation regions after annealing simulations. Tilings of the unit cells are shown. The quasicrystal tiles are: (P)entagon, (H)exagon, (N)onagon, (U)-tile, (D)ecagon, (Sq)are, (Tr)iangle, (Sh)ield.

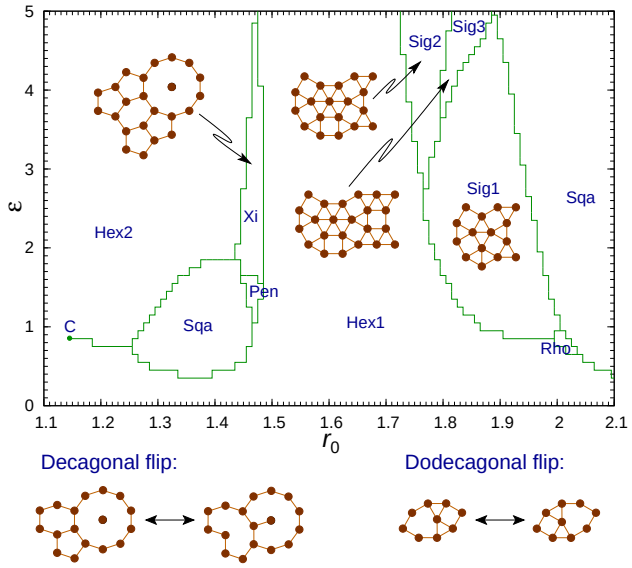

FIG. 3: (color online) Phase diagram of the LJG-potential at $T = 0$ with $\sigma^2 = 0.02$. Four approximants have been found. Phason flips correspond to local changes in the tilings.

by geometric constraints. Quasicrystals are not energetically stable at $T = 0$. The phase boundaries are slightly displaced compared to those from annealing simulations due to metastability.

The location of the stability regions can be understood from the near-neighbor configuration. Local n-fold order is stabilized for $r_0 \approx 2\cos(\pi/n)$. Fig. 3 confirms this except for local five-fold order, that is found at $r_0 \approx 1.47$ as a result of the competition with the close-packed phase

Phase	Density	Lattice constants	Atoms/u.c.
Pen	0.8981	$a = 2.62$, $b = 2.50$	5
Xi	0.7617	$a = 4.24$, $b = 4.24$	13
Dec	0.7608	—	—
Sig1	1.0718	$a = 2.73$, $b = 2.73$	8
Sig2	1.0788	$a = 3.73$, $b = 2.73$	11
Sig3	1.0829	$a = 4.73$, $b = 2.73$	14
Dod	1.0774	—	—

TABLE I: Structure details of the ideal tilings of the complex crystals. For comparison the quasicrystals are included.

Hex1. Structure details of the complex phases are collected in Tab. I: The phases Xi and Dec have a surprisingly low density, which is only 65% of the density of Hex1. They are locally very similar, their potential energies differ by less than 0.7%.

We have studied the decagonal quasicrystal in longer simulations using the parameters $r_0 = 1.52$, $\epsilon = 1.8$, and $\sigma^2 = 0.02$ (indicated by a cross in Fig. 2). With these parameters, the decagonal quasicrystal is assembled with few defects at elevated temperatures. A simulation of a large sample, 10000 particles, was initiated in a random configuration at $T = 0.50$, which is close to the melting point $T_M = 0.56 \pm 0.02$. In the following, the periodic boundary conditions are turned off to allow phason strain relaxation. At the beginning the particles quickly formed an amorphous state with local decagonal order. After about 10^5 molecular dynamics steps multiple grains with the quasicrystal started to grow. The bigger ones increased their size until at ca. 10^7 steps only one single grain remained. We continued the simulation up to $5 \cdot 10^7$ steps, healing out point defects (vacancies, interstitials) and improving the quasiperiodicity. At the end the sample was quenched to $T = 0$ and relaxed. The diffraction image (Fig. 4) shows a perfect decagonal symmetry with long-range order. There is a weak pattern of intrinsic diffuse scattering due to the randomness.

In the simulation the dynamics is dominated by particle jumps over the short distance $\Delta r = 0.6$, called phason flips, which transform energetically comparable configurations into another (see Fig. 3). Each such configuration can be mapped to a tiling and embedded as a discrete de Bruijn surface in a five-dimensional hypercubic lattice by noting that the tiling vertices are integer multiples of the five basis vectors $\boldsymbol{e}_n = (\cos(2\pi n/5), \sin(2\pi n/5))$. Although the average orientation of the surface is fixed by the decagonal symmetry, phason flips lead to local fluctuations $\boldsymbol{h}^\perp(\boldsymbol{r})$ in "perpendicular space" resulting in a phason strain $\chi_{ij} = \nabla_i h_j^\perp$. The ensemble of all accessible configurations forms a entropically stabilized random tiling with a phason elastic free energy density of the general form $f(T, \chi) = \lambda_1(T)\chi_1^2 + \lambda_2(T)\chi_2^2$, where χ_1^2, χ_2^2 are quadratic forms in χ_{ij}, and λ_1, λ_2 independent phason elastic constants [15].

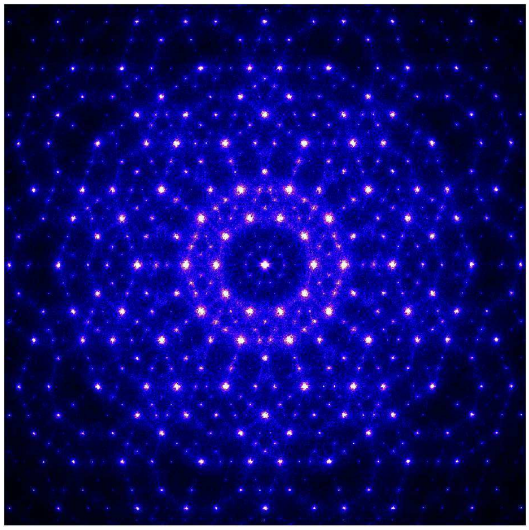

FIG. 4: (color online) Diffraction image of the large 10000 particle sample with the decagonal quasicrystal.

According to the $T = 0$ phase diagram a transformation to the phase Xi can occur during annealing [16]. This is achieved by (i) a collective rearrangement of the tiling induced by a global change of the de Bruijn surface orientation and (ii) a damping of the local phason fluctuations. For (i) to happen a huge number of phason flips is necessary, which makes the transition extremely slow. We performed long simulations over 10^9 steps with 1600 particles. At intermediate temperatures, $T < 0.40$, a reversible change in the tiling was found: The density of D-tiles increased and they arranged preferably close-packed in rhombs, characteristic for the approximant Xi. However as shown in Fig. 5, some defects and stacking faults were still present in the rhomb super-tiling.

At low temperatures, $T < 0.30$, the flip frequency was too slow to reach equilibrium with molecular dynamics. Hence we turned to a Monte Carlo algorithm, which allowed sampling the full temperature range from $T = 0.5$ down to zero and back up. As elementary step a random displacement inside a circle of radius 0.7 was used. The large radius allows both local relaxation and phason flips. The squared average phason strains χ_1^2, χ_2^2 are indicators of the de Bruijn surface orientation and thus order parameters for the phase transition. The results in Fig. 6 show a reversible transition at $T_c = 0.37 \pm 0.03$. Above T_c there is a strong increase in the density of D-tiles, which then slows down below T_c. The phason strains χ_1^2 and χ_2^2 fluctuate and switch from zero average at $T > T_c$ to finite values including a small hysteresis. We note that with periodic boundary conditions or in large samples phason flips alone cannot change the decagonal symmetry efficiently.

In the case of the Sig-phases, phason flips are not possible. They only occur in combination with Sh-tiles as

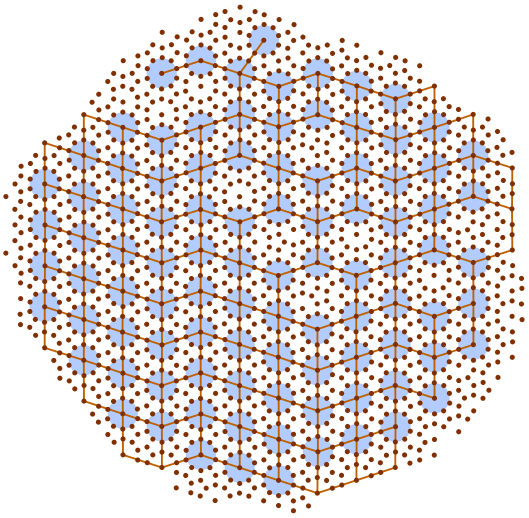

FIG. 5: (color online) Particle configuration in molecular dynamics simulation at $T = 0.30$. The D-tiles are arranged preferably in a rhomb super-tiling.

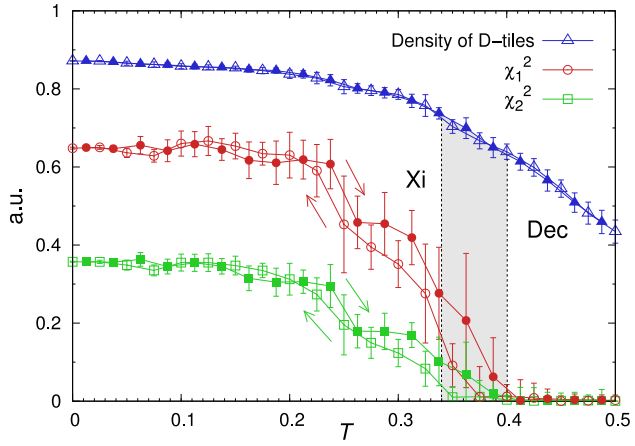

FIG. 6: (color online) Monte Carlo simulation of the phase transition between the decagonal RT and the approximant Xi. The data has been averaged over intermediate temperature intervals. Open symbols: cooling; full symbols: heating.

depicted in Fig. 3. Even though Sh-tiles are not seen in the ground states, they are present in equilibrium at higher temperature as structural defects. The flip mechanism then differs from the one in the decagonal RT [17].

Finally we comment on the value of the parameter σ and on other double-well potentials. The dynamics of the complex phases is controlled by the potential hill between the minima. A high potential hill leads to a low phason flip frequency and slow phase transitions, at least in molecular dynamics. On the other hand, a too low potential hill does not stabilize complex phases. The phase behavior is quite robust against small changes in the potential. Phase diagrams resembling Fig. 3 have been obtained for different values of σ. Choosing $\sigma^2 = 0.02$ constitutes a compromise between high flip frequency and stability. In contrast, the flip frequency of earlier models [7, 8] is much lower. Another example, a repulsive term plus two negative Gaussians has a qualitatively similar phase diagram, although additional phases appear. Further details will be presented elsewhere.

In conclusion, we have shown that systems with two competing nearest-neighbor distances can have a much more complicated phase behavior than what is known for single minimum potentials. Quasicrystals and complex crystals appear naturally in such systems as an attempt to maximize local particle configurations with non-crystallographic symmetry. In the presence of phason flips, entropic contributions to the free energy play an important role in the thermodynamic stability.

One of us (M.E.) would like to thank T. Odagaki for the hospitality during a stay at Kyushu University where part of this work was done. Financial support from the Deutsche Forschungsgemeinschaft under contract number TR 154/24-1 is gratefully acknowledged.

* Electronic address: mengel@itap.uni-stuttgart.de

[1] G. M. Whitesides and B. Grzybowski, Science **295**, 2418 (2002).
[2] P. Turchi and T. Massalski (editors), *The Science of Complex Alloy Phases* (TMS, Warrendale, 2005).
[3] K. Urban and M. Feuerbacher, J. Non-Cryst. Solids **334**, 143 (2004)
[4] C. Janot, *Quasicrystals: A Primer* (Oxford University Press, Oxford 1997).
[5] X. Zeng, G. Ungar, Y. Liu, V. Percec, A. E. Dulcey, and J. K. Hobbs, Nature **428**, 157 (2004).
[6] A. R. Denton and H. Löwen, Phys. Rev. Lett. **81**, 469 (1998).
[7] F. Lançon and L. Billard, Europhys. Lett. **2**, 625 (1986); J. Phys. (France) **49**, 249 (1988).
[8] M. Dzugutov, Phys. Rev. A **46**, R2984 (1992); Phys. Rev. Lett. **70**, 2924 (1993)
[9] J. Roth and A. R. Denton, Phys. Rev. E **61**, 6845 (2000).
[10] A. Quandt and M. P. Teter, Phys. Rev. B **59**, 8586 (1999).
[11] E. A. Jagla, Phys. Rev. E **58**, 1478 (1998).
[12] M. Rechtsman, F. Stillinger, and S. Torquato, Phys. Rev. E **73**, 011406 (2006).
[13] M. C. Rechtsman, F. H. Stillinger, and S. Torquato, Phys. Rev. Lett. **95**, 228301 (2005); Phys. Rev. E **74**, 021404 (2006); Phys. Rev. E **75**, 031403 (2007).
[14] J. Hafner, *From Hamiltonians to Phase Diagrams* (Springer-Verlag, Berlin, 1987); J. A. Moriarty and M. Widom, Phys. Rev. B **56**, 7905 (1997).
[15] M. Widom, D. P. Deng, and C. L. Henley, Phys. Rev. Lett. **63**, 310 (1989); K. J. Strandburg, L.-H. Tang, M. V. Jarić, Phys. Rev. Lett. **63**, 314 (1989).
[16] A quasicrystal-crystal phase transition in a similar model has been predicted by H. K. Lee, R. H. Swendsen, and M. Widom, Phys. Rev. B **64**, 224201 (2001).
[17] The elementary process is a zipper, see M. Oxborrow and C. L. Henley, Phys. Rev. B **48**, 6966 (1993).